Bacterial detachment from a wall with a bump line

doi: 10.1103/PhysRevE.99.023104

Bacterial detachment from a wall with a bump line

Jinyou Yang,[1,2,*] Yuji Shimogonya,[3] and Takuji Ishikawa[1,4]
[1]*Department of Biomedical Engineering, Graduate School of Biomedical Engineering, Tohoku University, 6-6-01 Aoba, Sendai 980-8579, Japan*
[2]*School of Fundamental Sciences, China Medical University, Shenyang 110122, China*
[3]*Department of Mechanical Engineering, Nihon University, 1 Nakagawara, Tokusada, Tamura, Koriyama 963-8642, Japan*
[4]*Department of Finemechanics, Graduate School of Engineering, Tohoku University, 6-6-01 Aoba, Sendai 980-8579, Japan*

(Received 14 November 2018; published 8 February 2019)

The interactions of bacteria with surfaces have important implications in numerous areas of research, such as bioenergy, biofilm, biofouling, and infection. Recently, several experimental studies have reported that the adhesion of bacteria can be reduced considerably by microscale wall features. To clarify the effect of wall configurations, we numerically investigated the behavior of swimming bacteria near a flat wall with a bump line. The results showed that the effects of bump configuration are significant; a detachment time larger than several seconds can be achieved in certain parameter sets. These results illustrate that the number density of bacteria near the wall may be reduced by appropriately controlling the parameter sets. When background shear flow was imposed, the near-wall bacterium mainly moved towards the vorticity axis. The detachment time of cells increased significantly by adjusting the bump line to have 45° relative to the flow direction. The knowledge obtained in this study is fundamental for understanding the interactions between bacteria and surfaces according to more complex geometries, and is useful for reducing the adhesion of cells to walls.

DOI: 10.1103/PhysRevE.99.023104

I. INTRODUCTION

Bacteria have occupied a broad range of ecological niches on Earth for billions of years. They represent the bulk of the world's biomass, even though they are the smallest organisms. Bacteria are responsible for many infectious diseases, yet they play a critical role in the life of soils and higher organisms, through chemical reactions and by providing nutrients [1,2]. In the wild, bacteria are predominantly associated with surfaces, and many of them rely on the presence of surfaces for their function and survival, e.g., bacteria biofilm formations on surfaces that enhance cell-cell exchange and nutrient uptake, as well as protect surfaces from external stresses [3].

In the field of biomaterials, interactions between bacteria and wall substrates have been investigated extensively. The interaction mechanism has been described in terms of the Derjaguin-Landau-Verwey-Overbeek (DLVO) theory of colloid stability [4,5]. Liu and Zhao [6] showed that the interaction can be attractive or repulsive, depending on the ratio of the Lifshitz–van der Waals apolar component to the electron donor surface energy components of the substrata. Some bacteria even secrete extracellular polymeric substances, which increases their affinity for heterogeneous surfaces [7,8].

The effect of hydrodynamics on bacterial adhesion has recently been emphasized [2,9]. Due to its small size, the flow field around bacteria can be described as Stokes flow, i.e., inertia less. Stokes flow impacts not only adhesion, but also many aspects of bacteriology such as the ability of cells to reorient and adjust to their surroundings [1]. For example, by imposing a vortical flow, Yazdi and Ardekani [10] experimentally demonstrated the formation of ring-shaped bacterial collection patterns, and subsequent formation of biofilm streamers in a microfluidic system. Fluid flow and the contact between cells and surfaces are two ubiquitous features influencing bacteria in natural environments [2].

In engineering, hydrodynamic interactions are utilized for designing microfluidic devices to control, manipulate, and separate bacteria [11–13]. DiLuzio *et al.* [14] showed that *Escherichia coli* (*E. coli*) bacteria in a microchannel swim preferentially along the right wall when confined to the bottom surface. By designing the appropriate wall configurations, bacteria trajectories can be controlled efficiently [15,16].

Recently, microscale wall surface patterns were found to decrease the adhesion of bacteria to walls. For example, Friedlander *et al.* [17] conducted a detailed investigation of how submicrometer crevices in a surface affect the attachment of *E. coli*. Feng *et al.* [18] reported that a nanoporous surface would effectively reduce bacterial attachment. Wall configurations are important in the interactions between bacteria and surfaces; information on these interactions will guide the development of new methods and materials that inhibit or promote cell growth and provide a better understanding of bacterial physiology in contact with surfaces [19].

Hydrodynamic interactions between bacteria and a flat wall have been clarified in detail [20]. Berke *et al.* [21] showed that the number density of *E. coli* near the wall was significantly higher than that in the bulk. In the vicinity of a flat wall, *E. coli* show a circling clockwise motion, which is a natural consequence of force- and torque-free swimming and the hydrodynamic interactions with the boundary [22–24]. *E. coli* produce circling counterclockwise motion when swimming

*yang@bfsl.mech.tohoku.ac.jp

near a liquid-air interface [25–27]. Some bacteria can become trapped in the corners of the channel wall by hydrodynamics [15,28]. Vizsnyiczai *et al.* [29] employed bumps on a surface to direct bacterial motion into a rotary machine above a surface. Although these studies are useful in understanding the aggregation and entrapment of cells near a flat wall, it is still unclear how bacteria can be detached from the wall. Several experimental studies have shown that the adhesion of bacteria can be reduced by changing the wall surface configuration [17,18,30]; however, a better understanding of the effect of wall configurations is required.

In this study, we investigated the effect of wall configuration on the detachment of a bacterium from the wall. We focused on the hydrodynamic interactions between the cell and the wall, and assumed a repulsive nature in the interactions between them, in an attempt to develop a wall configuration that had fewer cells compared with a flat wall. We computed the time duration required for the cell to become detached from the wall, i.e., the detachment time, using a boundary element method. The proposed wall configuration was a bump line on a flat wall.

The paper is organized as follows. In Sec. II, we explain the problem settings, basic equations, and numerical methods. The effect of the wall configuration on bacterial detachment is investigated in the absence of background flow in Sec III. In Sec. IV, we impose background shear flow, and discuss its effect. We present our conclusions in Sec. V.

II. METHODS

Hereafter, all quantities are nondimensionalized using characteristic length a^*, characteristic torque $\mathbf{T}^*_{\rm mot}$, and viscosity μ^* where a^* is the radius of a bacterium cell body, and $\mathbf{T}^*_{\rm mot}$ is the thrust torque required to rotate the flagellum. The symbol * represents a dimensional quantity; physical quantities without * represent dimensionless quantities.

A. Problem settings

We investigated the behavior of a bacterium swimming near a wall with a bump line. Figure 1 shows a schematic diagram of the problem settings. A flat wall is located at $z = 0$ in the rectangular coordinate system. The bump line is placed at $x = 0$ along the y axis, and the bump height is given by $z = \delta h[\frac{1}{2} - \frac{1}{2}\cos(2\pi\frac{x+\delta w/2}{\delta w})]$ in the range of $-\frac{\delta w}{2} \leqslant x \leqslant \frac{\delta w}{2}$, where δh is the maximum height at $x = 0$, and δw is the width of the bump.

A bacterium body is modeled as a spherical cell body with radius a, and a single helical flagellum with radius a_f, as in our former study [31]. Some bacteria have multiple flagella; however, the flagella usually form a bundle, e.g., *E. coli* bacteria [32]. Thus, we used a single rigid helix in this study. The position of any point along the centerline of the flagellum was derived by Higdon [33] and is given parametrically by

$$\mathrm{r}_f = \{s,\ h_f E_f(s)\cos(k_f s),\ h_f E_f(s)\sin(k_f s)\},$$
$$\text{with} \quad E_f(s) = 1 - \exp\left(-k_E^2 s^2\right), \tag{1}$$

where s is the coordinate along the flagellar axis, h_f is the amplitude, k_f is the wave number, and k_E is a constant that determines how quickly the helix grows to its maximum amplitude. In this study, as shown in Fig. 1, we used the following parameters to describe the bacterial shape: $2\pi/k_f = 2$, $h_f = 0.25$, $a_f = 0.1$, and $k_E = 1$.

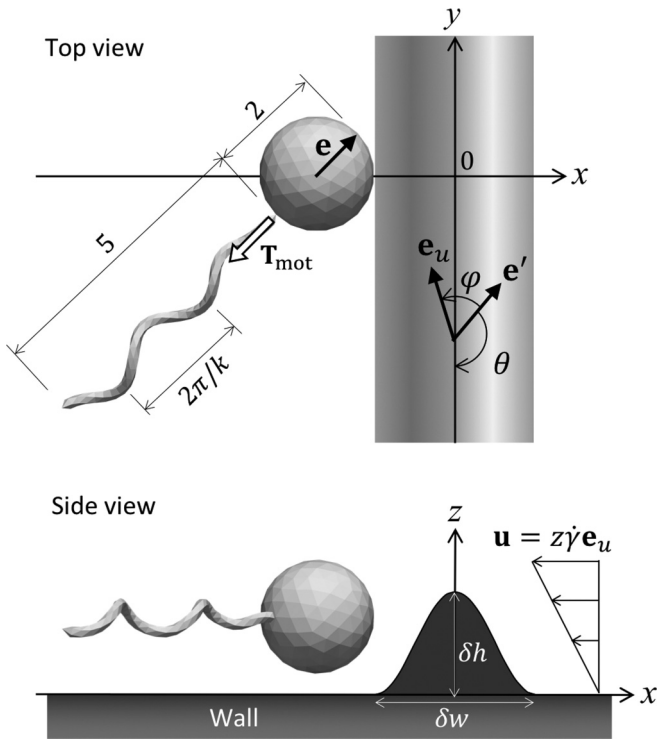

FIG. 1. Schematic diagram of the bacterial model and the problem settings. A flat wall exists at $z = 0$, and the bump line is aligned with the y axis. $\boldsymbol{e}$ is the unit orientation vector of the bacterium, and $\boldsymbol{e}'$ is the projection on the x-y plane. θ is the orientation angle relative to the bump line. Simple shear flow may be applied as $\boldsymbol{u} = \dot{\gamma} z \boldsymbol{e}_u$, where $\boldsymbol{e}_u$ is the direction of flow and $\dot{\gamma}$ is the shear rate. φ is the orientation angle relative to the shear flow. Bacterial shape parameters are set as $2\pi/k = 2.0$, h = 0.25, and the radius of the flagellum is $r_f = 0.1$.

The initial position of the center of the bacterial spherical body was placed at $\mathbf{x}_{c,t=0} = (-1 - \delta w/2,\ 0,\ 1.066)$. The initial height was determined so as to be the same as that providing a stable circular trajectory of the bacterium near a flat wall. Let the unit orientation vector of the bacterium be $\mathbf{e} = (e_x,\ e_y, e_z)$. We define the angle between the bacterium and the wall as $\theta = \arccos(-\mathbf{e}' \cdot \boldsymbol{n}_y)$, where $\mathbf{e}'$ is the unit projection vector of $\mathbf{e}$ on the x-y plane defined as $\mathbf{e}' = (e_x,\ e_y, 0)/\sqrt{e_x^2 + e_y^2}$, and $\boldsymbol{n}_y$ is the unit vector of the y axis. Initially, the bacterium is placed parallel to the wall at angle θ_0 with respect to the bump line, which was varied in this study.

In Sec. IV, we impose background shear flow. The unit vector in the flow direction is $\mathbf{e}_u$, and the flow field is given by $\mathbf{u}^\infty = \dot{\gamma} z \mathbf{e}_u$. The angle between the bacterium and the flow φ is defined as $\varphi = \arccos(\mathbf{e}' \cdot \mathbf{e}_u)$, as shown in Fig. 1, and its initial value is φ_0.

B. Basic equations

Due to the small size of a bacterium, we neglect inertial effects in the flow field and assume Stokes flow. In the Stokes flow regime, the velocity around the bacterium in integral

form [34] is given by

$$u_i(\mathbf{x}) - u_i^{\infty}(\mathbf{x}) = -\frac{1}{8\pi}\int_{\text{bacteria}} G_{ij}^{w}(\mathbf{x}-\mathbf{y})t_j(\mathbf{y})dA_c - \frac{1}{8\pi}\int_{\text{bump}} G_{ij}^{w}(\mathbf{x}-\mathbf{y})t_j(\mathbf{y})dA_b, \quad (2)$$

where $\mathbf{u}(\mathbf{x})$ is the velocity at position $\mathbf{x}$, $\mathbf{u}^{\infty}(\mathbf{x})$ is the background velocity, μ is the viscosity, A_c is the surface of the cell body and flagellum, A_b is the surface of the bump, and $\mathbf{t}$ is the traction force. The first integral on the right side is performed over the bacterial surface, while the second integral is performed over the bump line. $\mathbf{G}^{\text{w}}$ is the Green's function for the half space bounded by a no-slip wall, given by [35]

$$G_{ij}^{w}(\mathbf{x}-\mathbf{y}) = \left(\frac{\delta_{ij}}{r}+\frac{r_i r_j}{r^3}\right)-\left(\frac{\delta_{ij}}{R}+\frac{R_i R_j}{R^3}\right) + 2h(\delta_{j\alpha}\delta_{\alpha k}-\delta_{j3}\delta_{3k})\frac{\partial}{\partial R_k}\left\{\frac{hR_i}{R^3}-\left(\frac{\delta_{i3}}{R}+\frac{R_i R_3}{R^3}\right)\right\}, \quad (3)$$

where $\mathbf{y} = (y_1,\ y_2,\ h)$, $r = [(x_1-y_1)^2+(x_2-y_2)^2+(x_3-h)^2]^{1/2}$, $R = [(x_1-y_1)^2+(x_2-y_2)^2+(x_3+h)^2]^{1/2}$, and $\alpha = 1,\ 2$.

On the bump surface and on the wall, we apply a no-slip boundary condition. Rigid body motion is assumed for the bacterial cell body and flagellum. The flagellum is assumed to rotate relative to the cell body by a constant torque $\mathbf{T}_{\text{mot}}$ generated by a molecular motor. The torque is generated at the base of the flagellum in a direction normal to the cell body surface, as shown in Fig. 1. The motor torque should balance the hydrodynamic torque; thus, we have

$$-\mathbf{T}_{\text{mot}} = \int_{\text{flagellum}} (\mathbf{x}-\mathbf{x_a})\times\mathbf{t}(\mathbf{x})dA_f, \quad (4)$$

where the integral is over only the flagellum surface A_f, and $\mathbf{x_a}$ is the base position of the flagellum, i.e., the contact point between the spherical cell body and the flagellum. The bacterial model is assumed to be neutrally buoyant because the sedimentation velocity for typical aquatic bacteria is much less than the swimming speed. The center of buoyancy of the bacterium is assumed to coincide with its geometric center. Consequently, the model bacterium as a whole is force and torque free. Brownian motion is not considered, since typical bacteria have a body length, including flagella, of 2–10 μm [36] and are sufficiently large to neglect Brownian motion effects in the swimming behaviors around the bump. Thus, the force and torque equilibrium equations are given by

$$\mathbf{F} = \int_{\text{bacteria}} \mathbf{t}(\mathbf{x})dA_c = 0,$$
$$\mathbf{T} = \int_{\text{bacteria}} (\mathbf{x}-\mathbf{x_c})\times\mathbf{t}(\mathbf{x})dA_c = 0, \quad (5)$$

where the integral is over the whole bacterium surface, and $\mathbf{x_c}$ is the center of the cell body.

C. Numerical methods

The boundary element method was employed to discretize the governing equations, similar to the approach of Ishikawa *et al.* [31]. In total, 320 and 360 triangular elements were generated on the cell body and the flagellum, respectively.

Although the effect of a flat wall at $z = 0$ is taken into account by the Green's function, $\mathbf{G}^{\text{w}}$, that of the bump line is not. Thus, we generated a boundary element mesh along the bump line. The length of the bump line along the y axis was taken to be 108. Given that the effect of the bump decays with $1/d^2$ in Stokes flow near the wall, where d is the distance, a length of 108 is sufficiently large to ensure numerical accuracy. The mesh number, which depends on the distance between the bacterial surface and the bump surface, was chosen to optimize the numerical accuracy and computation time. The computational mesh on the bump consists of three sizes of triangles. When the distance between the bacterium and the bump is smaller than 0.4, the triangle has a side length of 0.2. When the distance between the bacterium and the bump is larger than 0.8, the triangle has a side length of 0.8. In between, the triangle has a side length of 0.4.

The surface integral in the basic equations was performed on the triangular element using 28-point Gaussian polynomials, and the singularity in the integration was solved analytically [37]. Time marching was performed using the fourth-order Adams-Bashforth method.

To express the repulsive nature of cell-wall interactions, we assumed a DLVO-type short-range repulsive force $\mathbf{F}_{\text{rep}}$, given by [38]

$$\mathbf{F}_{\text{rep}} = \alpha_1\frac{\exp(-\alpha_2\varepsilon_{\min})}{1-\exp(-\alpha_2\varepsilon_{\min})}\mathbf{d}, \quad (6)$$

where α_1 is a coefficient that controls the magnitude of the force, α_2 is a coefficient to control the decay length, $\varepsilon_{\min}$ is the minimum distance between the bacterial surface and the wall, and $\mathbf{d}$ is the unit vector connecting the minimum separation point from the wall. In this study, the coefficients were set as $\alpha_1 = \alpha_2 = 100$, such that the repulsive force is considerable when the minimum distance becomes smaller than about 0.01.

III. DETACHMENT OF A BACTERIUM IN THE ABSENCE OF BACKGROUND FLOW

A. Trajectories around the bump line

The behavior of a bacterium around the bump line was investigated. Typical trajectories are shown in Fig. 2. When the height of the bump was small, as in case A [Fig. 2(a)], the cell swam across the bump without changing the minimum separation distance $\varepsilon_{\min}$ considerably. If the cell swims across the bump, we refer to such a trajectory as "across." When the height of the bump is large, on the other hand, the cell cannot swim across the bump, but instead returns to the original side, as in case B [Fig. 2(b)], referred to as the "return" trajectory.

For a certain bump configuration, as in case C [Fig. 2(c)], the cell was directed upwards after the collision and detached from the wall. We define detachment when $\varepsilon_{\min}$ becomes larger than 0.2. We note that the initial value, as well as the stable value in a circular trajectory near a flat wall, were both $\varepsilon_{\min} = 0.066$. Figure 2(d) shows the time progression of $\varepsilon_{\min}$ for the three cases. The cells in cases B and C clearly detached from the wall. In case C, the cell swam away from the wall for thousands of time units. These results illustrate that a bacterium swimming near a wall can be detached from it by installing a bump line, which may eventually reduce the number density of bacteria near the wall.

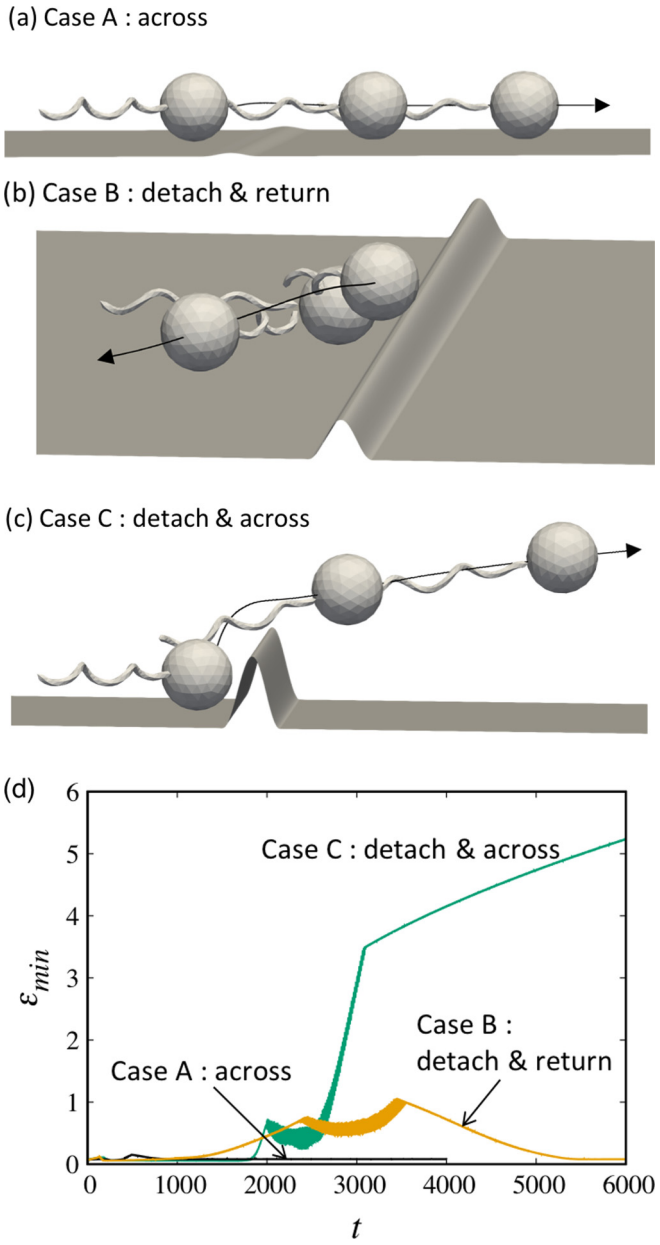

FIG. 2. Sample bacterial trajectories and the minimum distance between the wall and the bacterium. (a) Case A, a cell crossing the wall ($\delta h = 0.1, \delta w = 1.6, \theta_0 = 135°$); (b) case B, a cell detaching and returning from the wall ($\delta h = 1.0, \delta w = 1.6, \theta_0 = 90°$); and (c) case C, a cell detaching and crossing the wall ($\delta h = 2.0, \delta w = 1.6, \theta_0 = 135°$). (d) Time change of the minimum distance $\varepsilon_{\min}$ between the wall and the bacterium in cases A–C.

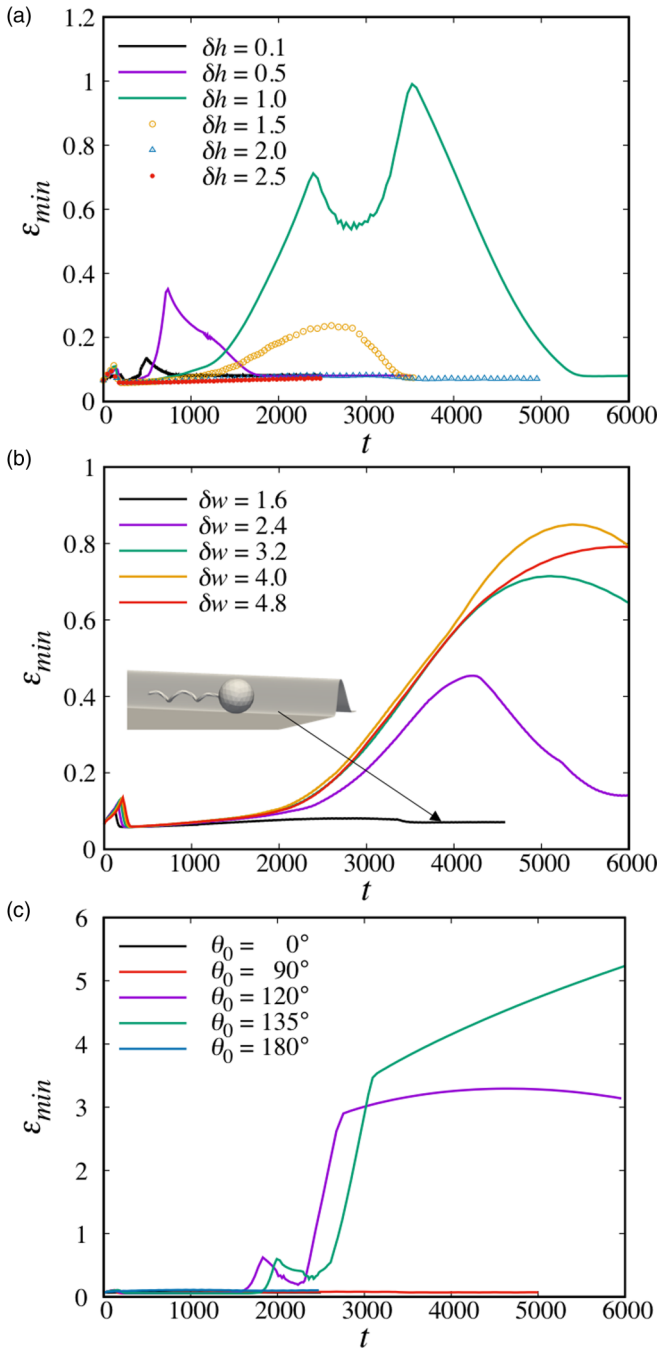

FIG. 3. Time change of the minimum distance $\varepsilon_{\min}$ between the wall and the bacterium. (a) Effect of the bump height δh ($\delta w = 1.6$, $\theta = 90°$). (b) Effect of the bump width δw($\delta h = 2.0$, $\theta_0 = 90°$). The inset indicates the final configuration of the bacterium in the case of $\delta w = 1.6$. (c) Effect of the initial orientation angle θ_0 ($\delta h = 2.0$, $\delta w = 1.6$).

B. Effect of wall configuration on detachment time

We also investigated the effect of the wall configuration on the detachment of a bacterium from the wall. Figure 3(a) shows the effect of bump height δh on the time change of the minimum separation distance $\varepsilon_{\min}$, under the conditions of $\delta w = 1.6$ and $\theta_0 = 90°$. We see from the figure that $\varepsilon_{\min}$ increased with δh, up to 1.0. These cells crossed the bump. When $\delta h = 2.0$ and 2.5, however, $\varepsilon_{\min}$ was small, and the cell swam close to the wall at all times. This is because the cell could return to the original side of the bump while swimming along it. The detachment, defined by $\varepsilon_{\min} \geqslant 0.2$, appeared when $0.5 \leqslant \delta h \leqslant 1.5$. These results indicate that there is an appropriate range of δh to induce cell detachment from the wall.

Figure 3(b) shows the effect of bump width δw on the time change of $\varepsilon_{\min}$, under conditions of $\delta h = 2$ and $\theta_0 = 90°$. We observed detachment when $\delta w \geqslant 2.4$, where these cells return to the original side of the bump. When $\delta w = 1.6$, the

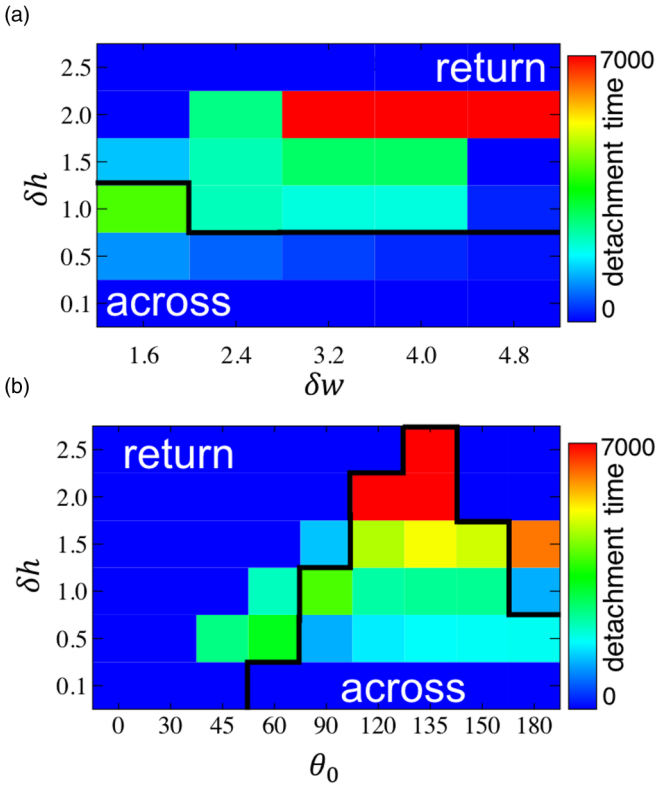

FIG. 4. Color contour of the detachment time. Black lines separate the behaviors of bacteria between across and return cases: (a) diagram plotted in δh–δw space with $\theta_0 = 90°$, and (b) diagram plotted in δh–θ_0 space with $\delta w = 1.6$.

cell stayed near the wall at all times. This is because the cell could not swim across the bump, and instead aggregated on the original side, as shown in the inset of the figure.

Figure 3(c) shows the effect of initial orientation angle θ_0 on the time change of $\varepsilon_{\min}$, under conditions of $\delta h = 2$ and $\delta w = 1.6$. We see that the effect of θ_0 is considerable. When $120° \leqslant \theta_0 \leqslant 135°$, the cell was apart from the wall for thousands of time units and crossed the bump. When $\theta_0 \leqslant 90°$ or $150° \leqslant \theta_0$, on the other hand, the cell stayed near the wall at all times. These results illustrate that the bump configuration and orientation angle have significant effects on the behavior of the bacterium near a wall.

Here we introduce the term "detachment time," which is the total time taken for a cell to satisfy $\varepsilon_{\min} \geqslant 0.2$. The effects of δh, δw, and θ_0 on the detachment time are shown in Fig. 4; the color indicates the length of the detachment time, and the black line separates the across and return cases (cf. Fig. 2). A large detachment time was found for both the across and return cases, so the classification may not be important when discussing the detachment time. The effects of δh, δw, and θ_0 are significant; a detachment time larger than 7000 can be achieved in certain parameter sets. These results illustrate that the number density of bacteria near the wall may be reduced by appropriately controlling the parameter sets. Although the wall configuration can be controlled during the fabrication process, controlling the orientation angle θ may not be as easy; e.g., in the absence of a background flow field, a bacterium near a wall may draw a circular trajectory, and the orientation angle θ may become arbitrary. In the next section, we consider background shear flow as a means of controlling θ.

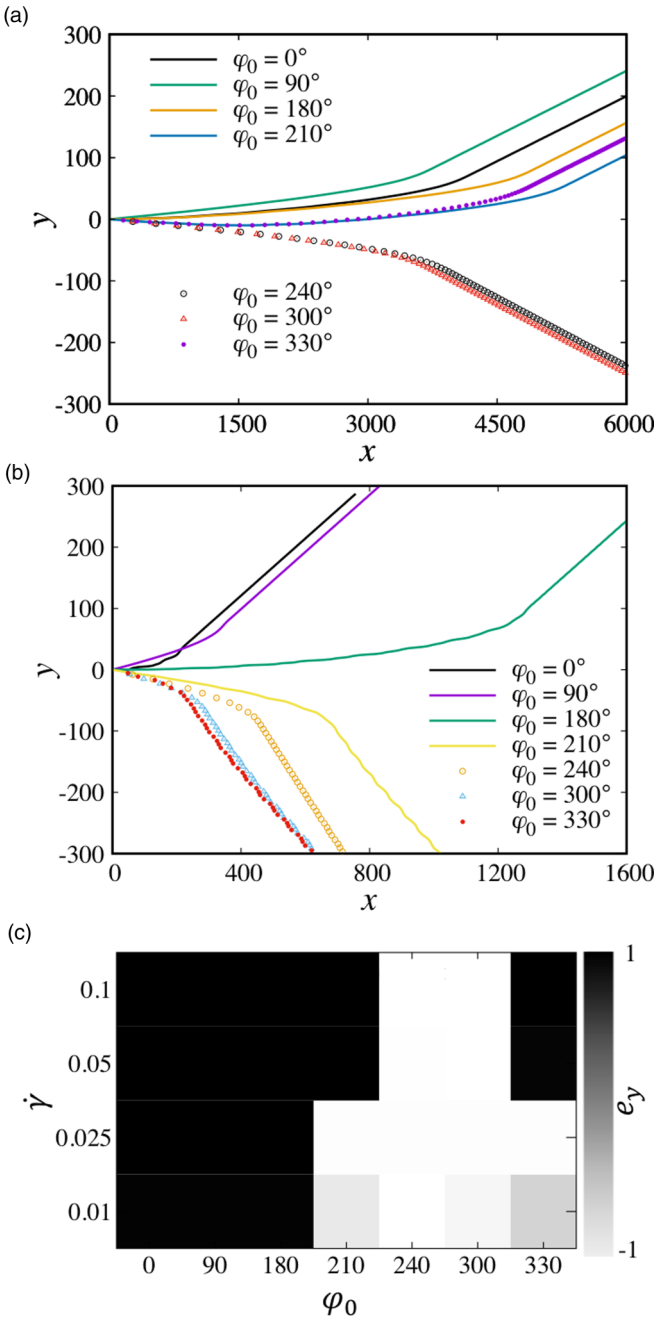

FIG. 5. Behaviors of bacteria in shear flow near a flat wall without the bump. Initially, the minimum distance was set as $\varepsilon_{\min} = 4.5$, and the orientation relative to the shear flow φ_0 was varied. (a) Trajectories with shear rate $\dot{\gamma} = 0.1$, (b) trajectories with $\dot{\gamma} = 0.01$, and (c) final orientation of bacteria as a function of $\dot{\gamma}$ and φ_0. $e_y = 1$ indicates that the bacterium is oriented with the positive y axis, whereas $e_y = -1$ indicates that the bacterium is oriented with the negative y axis.

IV. DETACHMENT OF A BACTERIUM IN BACKGROUND SHEAR FLOW

In nature and industries, biofilm can be formed under external fluid flow. In some engineering settings, such as in

a pipe, and in microfluidics, the flow directions are stable. Therefore, discussing the effect of the angle of the bump line relative to the flow direction should be useful in designing an effective wall configuration to reduce the number density of bacteria near the wall. In this section, therefore, we discuss detachment of a bacterium from a wall in simple shear flow.

A. Effect of shear flow in the absence of the bump

We first investigated the effect of shear flow on the bacterium swimming near a flat wall without a bump. The background flow was assumed to be simple shear flow; i.e., $\mathbf{u}^{\infty} = \dot{\gamma} z \mathbf{e}_u$. Here we take the x axis in the direction of $\mathbf{e}_u$, where $\dot{\gamma}$ is the shear rate, and is varied over the range of 0.01–0.1. Initially, the cell was placed parallel to the flat wall at a distance of 4.5 away from the wall, i.e., $\varepsilon_{\min} = 4.5$. The initial orientation angle relative to the flow direction φ_0 varied over the range of $0^{\circ} \leqslant \varphi_0 \leqslant 360^{\circ}$. The cell trajectory results are shown in Fig. 5. We see that cells do not swim straight, i.e., in the flow direction, but instead, drift to the side. The drift can be in the positive or negative y direction, depending on φ_0. Moreover, the trajectories change their slopes at certain downstream positions. This is because the cells eventually come close to the wall and change their orientation in the vicinity of the wall, which results in a change in the slope.

For both the $\dot{\gamma} = 0.01$ and 0.1 cases, the cells eventually become entrapped by the flat wall, despite being apart initially. This may explain why the trajectories are qualitatively similar in both cases. These results indicate that the cells naturally accumulate on the wall in the absence of the bump. These tendencies are consistent with the experimental observation of Berke *et al.* [21], in which *E. coli* were hydrodynamically attracted to a flat wall.

When the cells were entrapped by the flat wall, we found that most of them oriented in the positive or negative y direction, which is the reason why the cells did not swim straight but drifted to the side. The mechanism for a bacterium to orient in the vorticity direction is still under investigation, and we would like to clarify it in our future studies. Figure 5(c) shows the y component of the cell's orientation vector, when the cells were entrapped by the flat wall. We see that the value of e_y is $+1$ or -1 in most cases; thus, the cells were basically aligned with the y direction in shear flow. Such a tendency may be preferable, because the orientation angle θ relative to the bump line can be controlled once the flow direction is known.

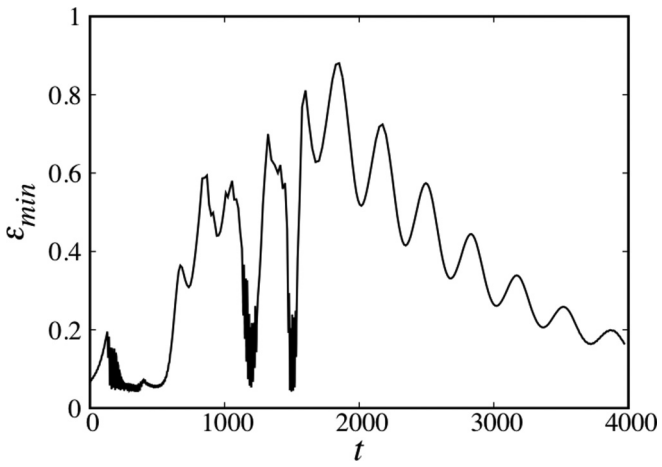

FIG. 6. Time change of the minimum separation distance $\varepsilon_{\min}$ with $\theta_0 = 90^{\circ}$. The shear rate is $\dot{\gamma} = 0.1$, and the bump configurations are $\delta w = 3.2$ and $\delta \mathrm{h} = 2.0$.

B. Bacterial detachment in shear flow

We now consider a bump line under shear flow conditions. When the flow direction $\mathbf{e}_u$ coincides with the direction of the bump line, all of the bacteria are directed perpendicular with respect to the bump line, as explained in the previous section. The wall configuration of $\delta h = 2$ and $\delta w = 3.2$ shown in Fig. 4(a) had the largest detachment time. Thus, by using the configuration, we investigated the trajectory of a bacterium with $\theta = 90^{\circ}$ in shear flow of $\dot{\gamma} = 0.1$. We found that the cell was elevated after the collision with the bump and detached from the wall in a manner similar to Fig. 2(c). Figure 6 shows that the detachment time was thousands of time units in this case.

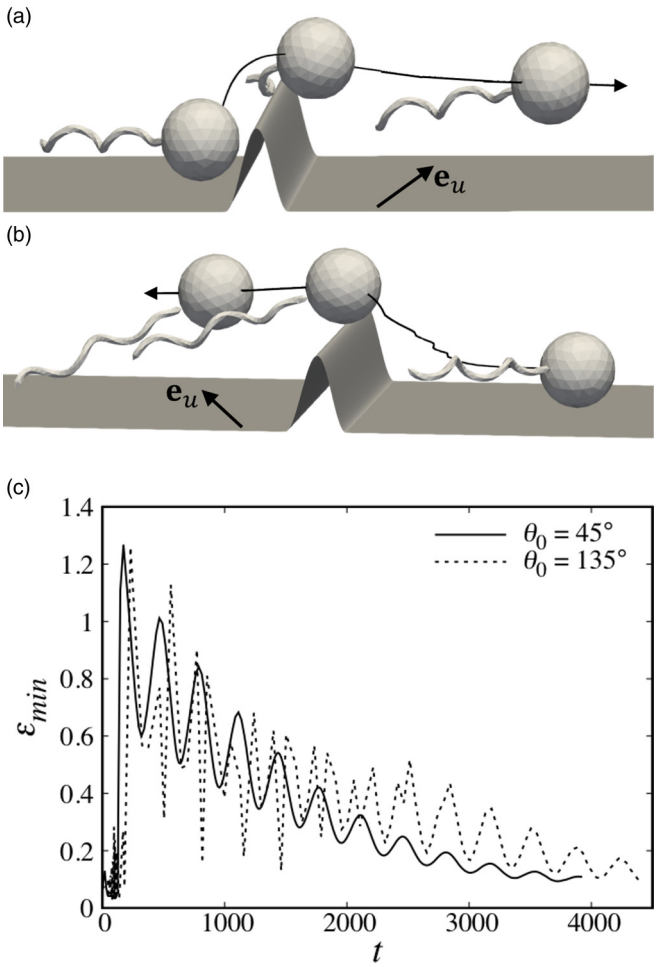

FIG. 7. Behavior of bacteria with $\theta_0 = 45^{\circ}$ and 135°. The shear rate is , and the bump configurations are $\delta w = 1.6$ and $\delta \mathrm{h} = 2.0$. (a) Trajectory and attitude of the bacterium with $\theta_0 = 45^{\circ}$. (b) Trajectory and attitude of the bacterium with $\theta_0 = 135^{\circ}$. (c) Time change of the minimum separation distance $\varepsilon_{\min}$.

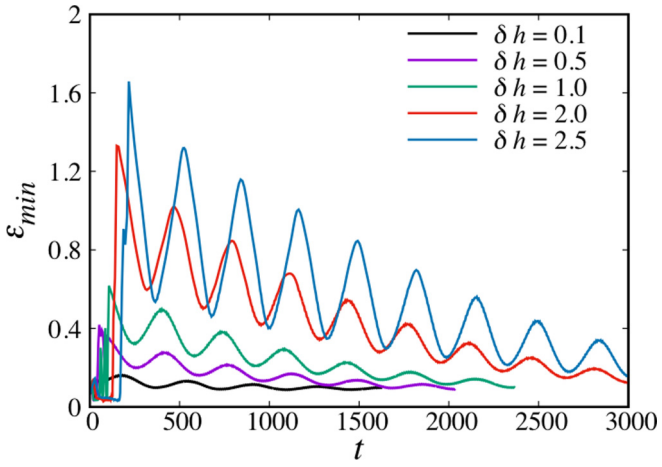

FIG. 8. Time change of the minimum separation distance $\varepsilon_{\min}$ of the bacteria with $\theta_0 = 45^\circ$. The height of the bump is varied from 0.1 to 2.5. The shear rate is $\dot{\gamma} = 0.1$, and the bump width is $\delta w = 1.6$.

In Fig. 4(b), a large detachment time was also observed with $\theta_0 = 135^\circ$. Thus, we calculated the trajectory of the bacterium with $\theta_0 = 135^\circ$ and $\dot{\gamma} = 0.1$ ($\delta w = 1.6$, $\delta h = 2.0$); the results are shown in Fig. 7(b): the cell was lifted up from the wall after the collision with the bump. Figure 7(c) shows that the cell detached from the wall for thousands of time units.

By imposing shear flow, a cell's orientation changes from the positive or negative y direction. When the bump line has an angle of $\theta_0 = 135^\circ$ for a cell with $e_y = 1$, the same bump has an angle of $\theta_0 = 45^\circ$ for a cell with $e_y = -1$. We thus also investigated the trajectory of the bacterium with $\theta_0 = 45^\circ$ and $\dot{\gamma} = 0.1$ ($\delta w = 1.6$, $\delta h = 2.0$). The results in Fig. 7(a) show that the cell was again lifted up from the wall after collision with the bump. Figure 7(c) shows that the cell detached from the wall for thousands of time units in both the $\theta_0 = 45^\circ$ and 135° cases. These results indicate that the wall with the bump line is capable of preventing a bacterium from attaching to the wall, even under shear flow conditions.

Figure 8 shows the effect of bump height δh on the time change of $\varepsilon_{\min}$ ($\theta_0 = 45^\circ$, $\dot{\gamma} = 0.1$, $\delta w = 1.6$). We see that $\varepsilon_{\min}$ and the detachment time increase as δh is increased. When $\delta h \geqslant 2.0$, the detachment time becomes thousands of time units. During 3000 time units, the bacterium in shear flow with $\dot{\gamma} = 0.1$ moved ~300 units downstream. If one installs parallel bump lines at interval lengths of 300, the bacterium could largely remain detached from the wall. Such a channel has a small number density of cells near the wall, which may reduce cell adhesion to the wall.

V. CONCLUSIONS

To clarify the effect of wall configurations on bacteria-wall interactions, we numerically investigated the behavior of a swimming bacterium near a flat wall with a bump line. This configuration was selected due to its simplicity and ability to detach bacteria from the wall.

Our results illustrate that a bacterium swimming near a wall can be detached from it by installing a bump line. The detachment time of a bacterium from the wall increased significantly, when the bump height δh is about 2 with certain parameter sets. As explained in Sec. II, the time unit can be dimensionalized as $t^* = t\mu^* a^{*3}/|\mathbf{T}^*_{\text{mot}}|$. By estimating the radius of the cell body to be $a^* = 1\,\mu$m, the characteristic torque to be $|\mathbf{T}^*_{\text{mot}}| = 10^{-18}$ N m, and the viscosity to be $\mu^* = 10^{-3}$ Pa s, one can derive that the dimensionless time duration of 1000 is equivalent to about 1 s. It indicates that a detachment time larger than several seconds was achieved in this study. When background shear flow was imposed, the near-wall bacterium was directed mainly to the vorticity axis. The detachment time of cells increased significantly by adjusting the bump line to have 45° relative to the flow direction. These results illustrate that the number density of bacteria near the wall may be reduced by appropriately controlling the wall configuration.

If parallel bump lines are installed at a certain interval, bacteria may be prevented from attaching to the wall. Such a channel has a small number density of cells near the wall, which may reduce the adhesion of cells to the wall. By estimating the radius of the cell body to be $a^* = 1\,\mu$m, interval lengths of about 300 μm may be efficient. The knowledge obtained in this study forms a fundamental basis for understanding the interactions between bacteria and surfaces in more complex geometries, and is useful for reducing cell adhesion to walls.

ACKNOWLEDGMENT

This research was supported by JSPS KAKENHI Grant No. 17H00853. The authors have no conflicts of interest regarding this paper.

[1] E. Lauga, Annu. Rev. Fluid Mech. **48**, 105 (2016).
[2] A. Persat, C. D. Nadell, M. K. Kim, F. Ingremeau, A. Siryaporn, K. Drescher, N. S. Wingreen, B. L. Bassler, Z. Gitai, and H. A. Stone, Cell **161**, 988 (2015).
[3] J. F. Lynch, H. M. Lappin-Scott, and J. W. Costerton, *Microbial Biofilms* (Cambridge University Press, Cambridge, UK, 2003).
[4] E. J. W. Verwey and J. T. G. Overbeek, *Theory of the Stability of Lyophobic Colloids* (Elsevier, Amsterdam, 1948).
[5] B. V. Derjaguin and L. D. Landau, Acta Phys. Chem. URSS **14**, 633 (1941).
[6] C. Liu and Q. Zhao, Biofouling **27**, 275 (2011).
[7] H.-C. Flemming and J. Wingender, Nat. Rev. Microbiol. **8**, 623 (2010).
[8] D. S. Spiegel and A. Burrows, Astrophys. J. **745**, 174 (2012).
[9] J. Elgeti and G. Gompper, Eur. Phys. J.: Spec. Top. **225**, 2333 (2016).
[10] S. Yazdi and A. M. Ardekani, Biomicrofluidics **6**, 044114 (2012).
[11] J. Elgeti, R. G. Winkler, and G. Gompper, Rep. Prog. Phys. **78**, 056601 (2015).

[12] S. E. Hulme, W. R. DiLuzio, S. S. Shevkoplyas, L. Turner, M. Mayer, H. C. Berg, and G. M. Whitesides, Lab Chip **8**, 1888 (2008).
[13] M. S. Davies Wykes, X. Zhong, J. Tong, T. Adachi, Y. Liu, L. Ristroph, M. D. Ward, M. J. Shelley, and J. Zhang, Soft Matter **13**, 4681 (2017).
[14] W. R. DiLuzio, L. Turner, M. Mayer, P. Garstecki, D. B. Weibel, H. C. Berg, and G. M. Whitesides, Nature **435**, 1271 (2005).
[15] P. Galajda, J. Keymer, P. Chaikin, and R. Austin, J. Bacteriol. **189**, 8704 (2007).
[16] T. Ishikawa, T. Shioiri, K. Numayama-Tsuruta, H. Ueno, Y. Imai, and T. Yamaguchi, Lab Chip **14**, 1023 (2014).
[17] R. S. Friedlander, H. Vlamakis, P. Kim, M. Khan, R. Kolter, and J. Aizenberg, Proc. Natl. Acad. Sci. U. S. A. **110**, 5624 (2013).
[18] G. Feng, Y. Cheng, S.-Y. Wang, D. A. Borca-Tasciuc, R. W. Worobo, and C. I. Moraru, npj Biofilms Microbiomes **1**, 15022 (2015).
[19] H. H. Tuson and D. B. Weibel, Soft Matter **9**, 4368 (2013).
[20] E. Lauga and T. R. Powers, Rep. Prog. Phys. **72**, 096601 (2009).
[21] A. P. Berke, L. Turner, H. C. Berg, and E. Lauga, Phys. Rev. Lett. **101**, 038102 (2008).
[22] E. Lauga, W. R. DiLuzio, G. M. Whitesides, and H. A. Stone, Biophys. J. **90**, 400 (2006).
[23] H. Shum and E. A. Gaffney, Phys. Rev. E **91**, 033012 (2015).
[24] D. Giacché, T. Ishikawa, and T. Yamaguchi, Phys. Rev. E **82**, 056309 (2010).
[25] L. Lemelle, J.-F. Palierne, E. Chatre, and C. Place, J. Bacteriol. **192**, 6307 (2010).
[26] J. Hu, A. Wysocki, R. G. Winkler, and G. Gompper, Sci. Rep. **5**, 9586 (2015).
[27] R. Di Leonardo, D. Dell'Arciprete, L. Angelani, and V. Iebba, Phys. Rev. Lett. **106**, 038101 (2011).
[28] H. Shum and E. A. Gaffney, Phys. Rev. E **92**, 063016 (2015).
[29] G. Vizsnyiczai, G. Frangipane, C. Maggi, F. Saglimbeni, S. Bianchi, and R. Di Leonardo, Nat. Commun. **8**, 15974 (2017).
[30] R. J. Crawford, H. K. Webb, V. K. Truong, J. Hasan, and E. P. Ivanova, Adv. Colloid Interface Sci. **179–182**, 142 (2012).
[31] T. Ishikawa, G. Sekiya, Y. Imai, and T. Yamaguchi, Biophys. J. **93**, 2217 (2007).
[32] H. C. Berg, *Random Walks in Biology* (Princeton University Press, Princeton, NJ, 1993).
[33] J. J. L. Higdon, J. Fluid Mech. **94**, 331 (1979).
[34] C. Pozrikidis, *Boundary Integral and Singularity Methods for Linearized Viscous Flow* (Cambridge University Press, Cambridge, 1992).
[35] J. R. Blake and A. T. Chwang, J. Eng. Math. **8**, 23 (1974).
[36] C Brennen and H. Winet, Annu. Rev. Fluid Mech. **9**, 339 (1977).
[37] G. K. Youngren and A. Acrivos, J. Fluid Mech. **69**, 377 (1975).
[38] T. Ishikawa and T. J. Pedley, J. Fluid Mech. **588**, 437 (2007).